Simulation of electromagnetically formed joints

R. Neugebauer[1], V. Psyk[1], C. Scheffler[2]

[1] Fraunhofer Institute of Machine Tools and Forming Technology, Chemnitz, Germany
[2] Institute for Machine Tools and Forming Technology, Chemnitz University of Technology, Germany

Abstract

The most important application of electromagnetic forming (EMF) is joining by compression of tubular workpieces. The process simulation of such high speed forming steps must consider numerous mechanical, electrical, and electro-magnetic material characteristics and sometimes a even thermal dependency generally resulting in highly nonlinear computations. One of the most important interactions of the physical fields is the mutual dependency between the acting loads and the deformation. Consequently, a coupled field simulation of structure and magnetic field is demanded. In this paper an exemplary industrial joint produced by EMF is regarded. By comparative electromagnetic field simulations it is proved that the influence of the non-linear permeability of ferromagnetic materials in EM-forming problems is small. A three-dimensional coupled simulation of the joining process is carried out by help of an EM-module in a beta version of the LS-DYNA structural explicit code. To evaluate the quality of the resulting joint already in the virtual process design, the maximum transmittable moment is computed. An experimental verification of the forming and the testing procedure concludes the paper.

Keywords

Electromagnetic forming, Coupled Simulation, Strain rate, Permeability

1 Introduction

Already in the 1970s Bühler et al. claimed joining of tubular components to be the most promising application field of electromagnetic forming (EMF) [1] and this trend has not changed up to now. A comprehensive overview of literature related to EMF including early work as well as recent publications about joining by EMF is given in [2]. As mentioned in this survey, tubes and hollow profiles can be connected to an outer joining partner (hub) by expansion or to an inner joining partner (mandrel or shaft) by compression, whereby the latter case is more common.

Depending on material and shape of the components as well as on the process parameters the resulting joining mechanism can be based on interference-fit, form-fit, metallic bonding, or a combination of the mentioned types [3]. Provided that the joint is properly designed and the process parameters are carefully chosen, all joining mechanisms allow manufacturing connections with a strength comparable to that of the parent material. In case of interference-fit joints, the transferable load depends on the friction coefficient, the pressure in the contact zone and the size of the contact zone. To increase the transferable load sometimes the joining area has to be chosen rather large. In practical applications this might contradict design aspects or requirements resulting from lightweight construction concepts. Contrary, form-fit joints and metallically bonded connections can often transfer the required load via a smaller joining zone. However, the required energy for metallic bonding is rather high, so that with regard to energy efficiency in many cases form-fit joining is the best alternative.

For this type of joint the shaft and the hub, respectively features geometrical elements as grooves or beads. During the process the tubular joining partner is deformed and the material flows into the geometry element forming an undercut. As discussed in [2]and [4], the influence of the groove geometry on the transferrable load has been investigated by numerous authors, setting the main focus on axial loading of the joint, exclusively. However, in many practical applications profile shaped components and the related joints accordingly are loaded by torque. Thus, the current paper focuses on form-fit joints produced by electromagnetic compression and the related strength considering torsion-loading. In Figure 1 an examplary industrial joint from the automotive sector is presented. Here, a steel tube made of C35 with a diameter of 42.4 mm and a wall thickness of 3.2 mm is connected to a steel shaft made of C45. To optimize the joint with regard to this torque loading, different axially oriented geometry elements have been tested. For the analysis a combined numerical and experimental investigation strategy has been chosen.

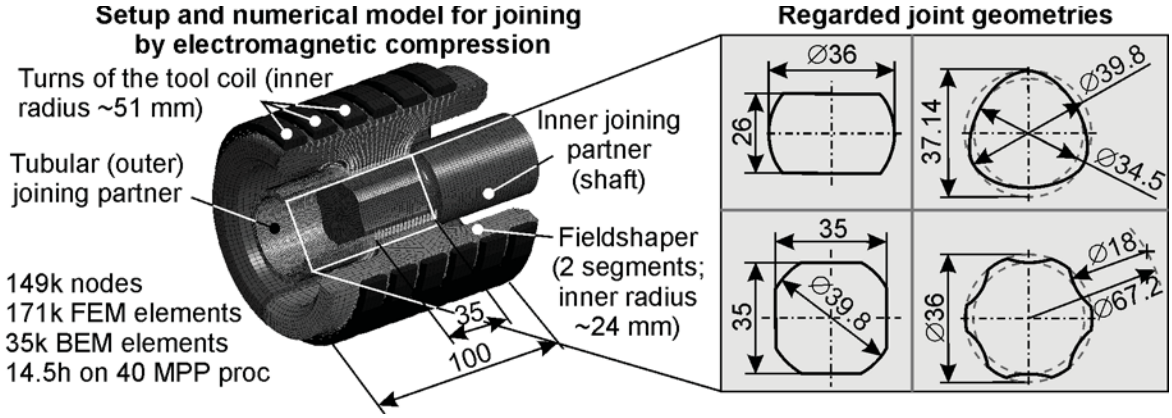

Figure 1: *Examplary industrial application of joining by electromagnetic compression.*

2 Principle and Simulation of Electromagnetic Forming

In electromagnetic forming the energy density of a pulsed magnetic field is used for applying a so-called magnetic pressure to workpieces made of electrically conductive material. In a compression process the tool coil surrounds the tubular workpiece. As

illustrated in Figure 1 the setup can be completed by a so-called fieldshaper and for joining purposes a joining partner is positioned inside the workpiece. Discharging a capacitor battery through the coil leads to a damped sinusoidal coil current and an according magnetic field which extends mainly in the air gaps between coil and fieldshaper, the individual fieldshaper segments, and fieldshaper and workpiece. Due to the deformation of the tube, the gap volume increases and consequently the energy density i.e. the magnetic pressure that is the source of the deformation decreases.

This interdependency between acting loads and resulting workpiece deformation is one of the most important points when simulating EMF and related joining or cutting processes. To obtain an accurate model of the complete process, different physical effects as mechanical material characteristics like the strain rate dependant flow curve, electrical and electro-magnetic properties and in some cases even a thermal dependency have to be considered, generally resulting in highly nonlinear computations. Consequently, the simulation of EMF is an extremely complex problem and numerous authors have been presenting different numerical simulation tools to solve it (e.g. [5]-[8]). Details about these developments can be found e.g. in [2].

Although many of the described simulation tools include the most important physical aspects and lead to good qualitative and quantitative results as verified in experimental investigations, up to now a fully developed and commercially available solution is still lacking. Consdidering this special aspect, the developments of L'Epplattenier et al. (see [9]) have currently reached the highest stage of development and have been used successfully by many researchers. Similarly, also in this work the numerical analysis of the joining process is based on this tool offering the additional benefit of performing the torque simulation directly after EMF keeping the initial stress / strain in the elements.

3 Simulation

3.1 Permeability influence

In the work mentioned above mainly workpieces made of aluminium alloys are regarded. One reason for this is the their high electrical conductivity which enables high process efficiency during EMF. However, in industrial applications steel materials have been and will continue being used frequently and requests for forming and joining steel by EMF are common despite of the comparably low electrical conductivity. Thus, the influence of the ferromagnetic properties of many steels is an issue in the electromagnetic simulation.

One aspect is the magnetic hysteresis which exists in particular for steel materials because of the high energy dissipation caused through the reversal of magnetization. In general this is difficult to model due to the dependency on the material history (similar to plastic material behavior in continuum mechanics). However, as it can be seen from Figure 2, hysteresis is not significant in the field intensity range usually used for EMF and that is why it is rightfully neglected in many cases.

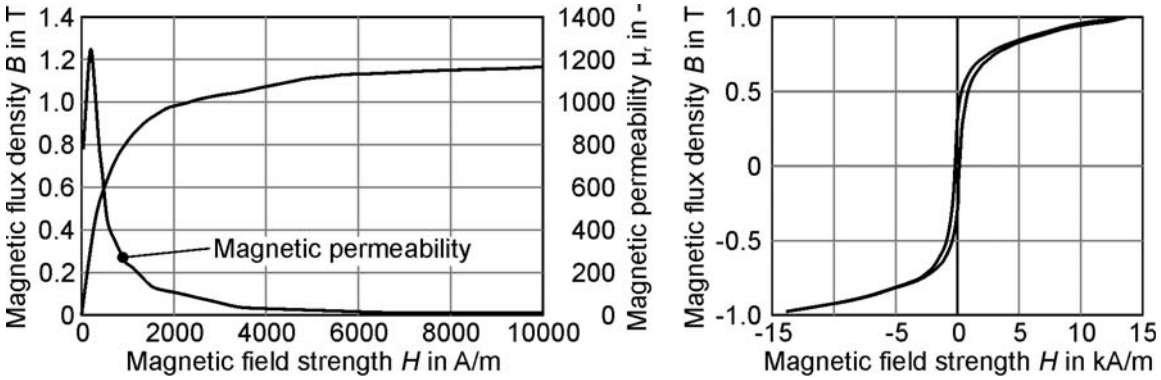

Figure 2: *Left: Nonlinear B-H characteristic (magnetization curve) used in the simulation and computed relative permeability. Right: Hysteresis curve of an unalloyed steel [10].*

In most of the EMF simulations simplifications considering the relative permeability μ_r are made. Assuming that it is isotropic, is valid in most cases and therefore not reviewed, here. Accordingly the μ_r tensor of second order becomes a scalar.

Moreover, the permeability is often neglected or considered as constant. To investigate if this simplification is admissible for EMF, a magnetic nonlinear simulation with the model described above was set up in ANSYS. An imposed current of 50 kA and a frequency of 10 kHz (both are typical values for EMF) were assumed and axisymmetric plane 233 elements with a nodal based magnetic vector potential formulation were used.

In Figure 2 a typical initial magnetization curve of a steel, similar to C35E, is displayed. The relation of H-dependency and isotropic, i.e. scalar, permeability is given by

$$d\mathbf{B}(H) = \mu_r(H)\mu_0 d\mathbf{H} \tag{1}$$

where **H** is the magnetic field intensity vector (H the norm of **H**), **B** the magnetic field density vector, μ_r the isotropic relative permeability and μ_0 the magnetic field constant $4\pi \cdot 10^{-7}$H/m. By plotting the computed μ_r over it becomes obvious that μ_r varies between 1 and about 1200 (see Figure 2). Due to magnetic saturation the permeability tends to 1 for high values of the field intensity. According to [11], the maximum of permeability is shifted to higher H-values if the carbon portion is increased and if the material is hardened but they are still much lower than the typical magnitude during EMF which is in the range of 10^5 up to 10^8 depending on the current, coil and tool geometry as shown in Figure 3.

Thus, it can be expected that the magnetic material behavior is in good approximation linear with μ_r=1. This assumption was proofed by comparisons of field lines or the spatially distributed μ_r-values. The field line plots for linear and nonlinear magnetization shown in Figure 3 (for reasons of symmetry only one quarter of the cross section is shown, here) do not differ significantly from each other implying a great similarity of the fields. This becomes obvious as well by depicting the computed μ_r over the modelling region (Figure 4). For high current amplitudes (i.e. approx. 30-200 kA) μ_r is equal 1 almost everywhere in the workpiece and the tool has no influence (see Figure 4a).

Contrary, for smaller currents (e.g. a 5 kA amplitude) a permeability distribution in the workpiece with values >>1 results (see Figure 4b) implying a mandatory consideration of nonlinear magnetization, but usually such small currents are not relevant in EMF.

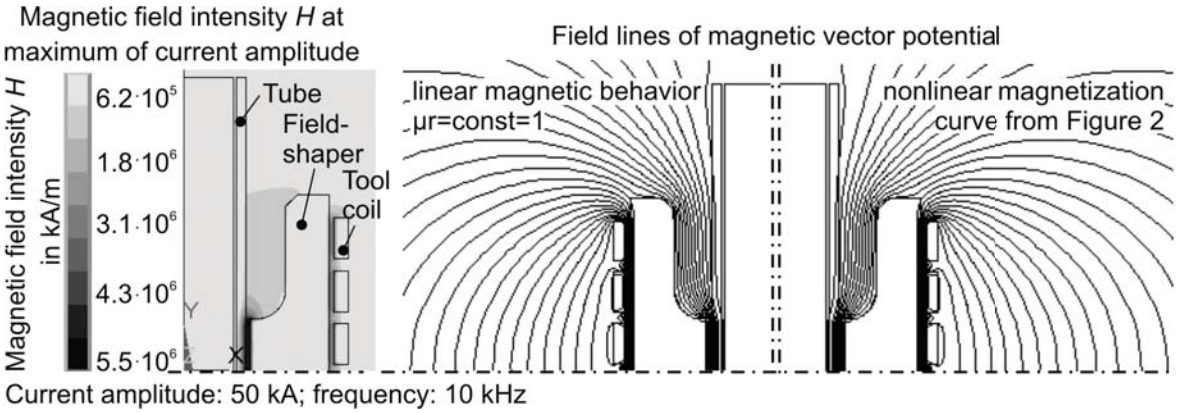

***Figure 3**: Typical magnetic field intensity H and Field lines of magnetic vector potential for linear (left) and nonlinear (right) magnetic behavior.*

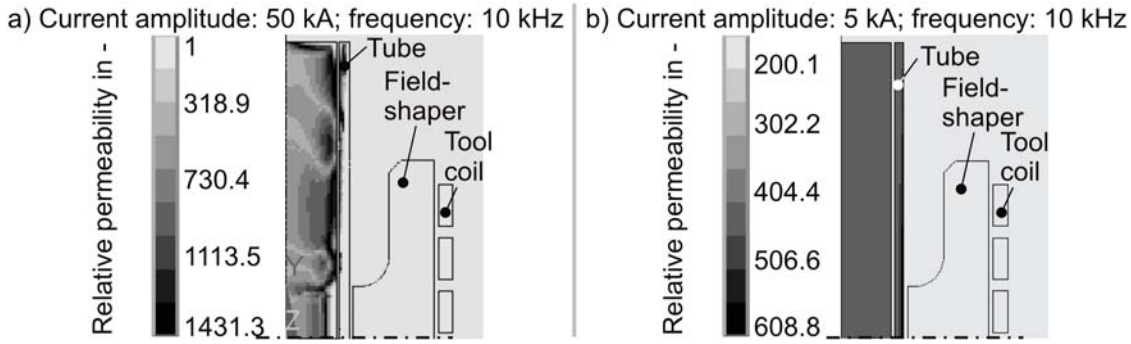

***Figure 4**: Distribution of the relative permeability μ_r (non-linear magnetization curve according to Figure 2). Regions with high values of H (Figure 3 a) and current densities, what means there exist high Lorentz forces, have μ_r values near 1.*

It can be concluded that for EMF simulations it is not necessary to deliberate whether to consider permeability effects or not. They have minor influence than other simplifications or assumptions within the modelling as e.g. uncertainties for electrical, magnetic or structural material parameters.

3.2 Modelling of strain rate dependency

Different kinds of material models are used for describing the strain rate dependency on the flow stress. These are mainly empirical models based on a phenomenological approach like the Cowper-Symonds-, or the more modern Johnson-Cook model (*MAT_24 and *MAT_15), which are widely used in FEM simulations. Semi-empirical (e.g. the Zerilli-Armstrong model, *MAT_65 in LS-DYNA) or physically motivated models are not so popular in FEM-simulations.

It turned out that the strain rate dependency is significant for steel materials and in particular for the high strain rates occuring in EMF. The magnitude of these values is exemplarily shown in Figure 5. Therefore, we consider the scaling of the static yield stress σ_y^s in the coupled electromagnetic-structural forming simulation in a tabulated way $\sigma_y\left(\varepsilon_{eff}^p, \dot{\varepsilon}_{eff}^p\right) = \sigma_y^s\left(\varepsilon_{eff}^p\right) \cdot f\left(\dot{\varepsilon}_{eff}^p\right)$ based on given data for C45 [7].

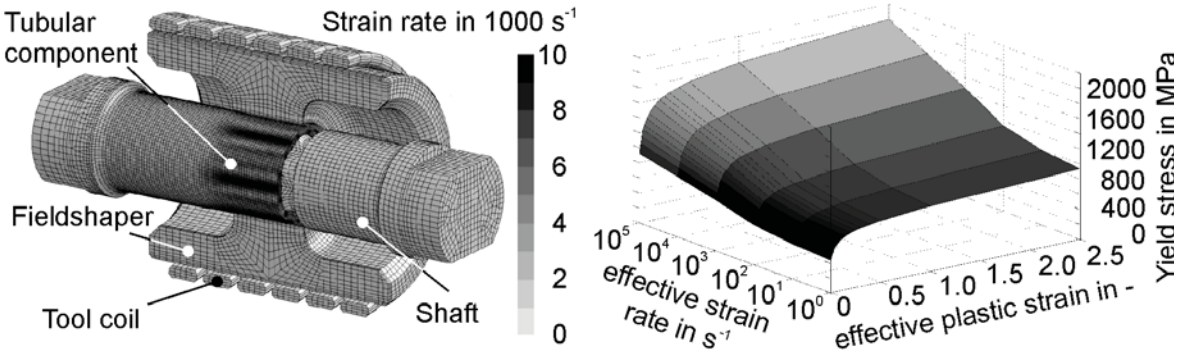

***Figure 5**: Left: Strain rate distribution during EMF. Maximum values are around 16000s^{-1}. Right: Scaling factor for the static yield stress considering strain rate dependency.*

3.3 Coupled Electromagnetic Simulation

One essential step forwards in electromagnetic field simulation is the coupling of the electromagnetic equations with the structural equations. In the LS-DYNA 980 beta version, an electromagnetism module (EM) is under development, which allows the coupled computing of highly nonlinear transient problems in time domain [9]. Furthermore, the explicit structural solver is particularly suitable to handle problems, like EMF, with physical (material) and geometric (contact) nonlinearities.

The FEM approach of this EM-Module bases on a method which was developed by Rieben et. al. [12] and uses a new high-order spatial discretization for the finite element problem. This FEM approach was later introduced in the FEMSTER package [13] which provides a general modular FE class library for hexahedrons, prisms and tetrahedrons. Because of the correct modelling of conditions like jump discontinuities and the divergence-free properties of the magnetic and electric fields together with the implicit unconditionally stable time integration algorithm which is charge and energy conservative, this mixed finite element method is perfectly suited for the time dependent coupled Maxwell equations, i.e. the Ampere and Faraday law.

Another characteristic in LS-DYNA's EM-module is the use of a special boundary element (BEM) formulation known as indirect BEM for solving the Maxwell equations in insulator regions, i.e. regions without (eddy) currents. Thus, meshing of non-conductors like the air is not necessary preventing element distortion during forming. The BEM-formulation of air is particularly suitable due to the linear magnetic characteristic (μ_r=1).

A coupling to the mechanical equations is applied in every time step by help of the computed Lorentz force which acts on the nodes of the mesh. This can be regarded as weak coupling. To consider the feedback of the deformed structure on the magnetic field the FEM and BEM matrices of the magnetic equation system are recomputed in every n-th mechanical timestep. The frequency of the matrix update depends on the influence of the deformed structure and can often be set around every 100th mechanical timestep because of the small mechanical steps in explicit FEM dynamics.

There exist several formulations for solving the electromagnetic field equations [14]. On of the most common is the A, φ-A formulation, what means to describe the Maxwell equations for insulator regions through the magnetic vector potential A and for conductive regions through the magnetic vector potential + the electric scalar potential φ. Thus, the constraints (e.g. the divergence condition) could be incorporated easily and the number of

constraints is reduced. Additionally, some simplifications can be applied, like the so-called eddy current approximation by neglecting the displacement current (valid in every case of EMF because wave propagation does not play a roll) and the assumption of the absence of free charges in EM domain.

The mixed finite element formulation for FEM and BEM means that for the element shape and weighting functions different basis functions dependent of the quantities are used for discretization of the field equations. It is both a nodal based formulation like widely used and as well an edge, surface and volume related formulation. 0. order basis functions are scalar and used for the discretization of scalar values on the nodes of the mesh like the electric scalar potential. First order basis functions are vector basis functions and used for discretization of quantities which have continuous tangential constraints on the edge of elements, like it is necessary for the magnetic field intensity or the magnetic vector potential. These basis functions satisfy exactly numerical relations such as *rot grad* φ*=0* or *div rot H=0* which occur in conservation laws of the electromagnetic field equations.

The disadvantage of the applied BEM formulation is that in its original form it produces (fully) dense matrices which results in both a time consuming assembling and requires large memory space. In order to reduce the computational costs, methods related to the Fast Multipol Method (FMM) are applied for solving the special integrals with potential characteristic which occur during the BEM matrices assembling. One more advantage is that the matrix assembly is perfectly suited for parallelization (matrix entries = integrals can be computed absolutely separate).

3.3.1 Model and results

The model was build up in LS-DYNA by help of advanced meshing tools like ANSA to ensure both an appropriate mesh for the electromagnetic problem and for the mechanical forming and subsequent torque simulation with a sufficient fine volume discretization. The model in Figure 1, consists of the components coil, field shaper, tube and shaft; the latter one with different geometries. The material characteristic of tube and shaft was modelled with an isotropic plastic material with a given stress-strain curve, considering the strain rate dependency by a scaling factor for the yield stress (see Figure 5), and for the field shaper with an elastic material because the stress was expected below the yield strength. The coil was modelled as rigid. Based on the results from the permeability consideration, the magnetic characteristic was, simplified by linear magnetic behavior or even neglected for the shaft because the high wall thickness clear more the penetration depth of the magnetic field. The penetration constant for C35E steel is given at about 12.5 kHz discharging frequency (see Figure 6) to $\delta = (\sigma \mu_0 \pi f)^{-1/2} = 0.74mm$. The pulse unit characteristic was modeled by a capacitance of 330 µF, an inductance of 150 nH, and a resistance of 5 mΩ with a used capacitor voltage of 16 kV.

Important results of the numerical investigations of the two best joint geometries are depicted in Figure 6 in form of the history of the coil current and inductance. Both show steps which are caused by the workpiece deformation and a recomputation of the BEM matrices after every 7µs. Due to deformation the air gap is increased and the inductance increased as well to what is reasonable.

	Coil	Field shaper	Shaft	Tube	Insulator+Air
Material	CuZr	CuZr	C45E	C35E	-
Mechanical parameters					
Mechanical behavior	rigid	elastic	elastic-plastic, strain rate dep.	elastic-plastic, strain rate dep.	-
Density ρ [kg/dm³]	-	8.75	7.85	7.85	-
Friction value μ_r [-]	-	-	0.12		-
Magnetic parameters					
Magnetic behavior	linear	linear	-	linear	linear
Approximation	eddy-current	eddy-current	-	eddy-currents	no eddy currents
Rel. permeability μ_r [-]	1.0	1.0	-	1.0	1.0
Conductivity σ [Ω⁻¹m⁻¹]	$3.7 \cdot 10^7$	$3.7 \cdot 10^7$	-	$0.5 \cdot 10^7$	0.0

Table 1: *Material parameters*

The magnitude of the inductance step already allows qualitative conclusions regarding the deformation. The higher steps after 21 µs and 28 µs indicated more deformation in case of the joint geometry 1 at the beginning of the process while at the end the joint geometry 2 is deformed more. The final geometry determined in the simulation is depicted in Figure 7.

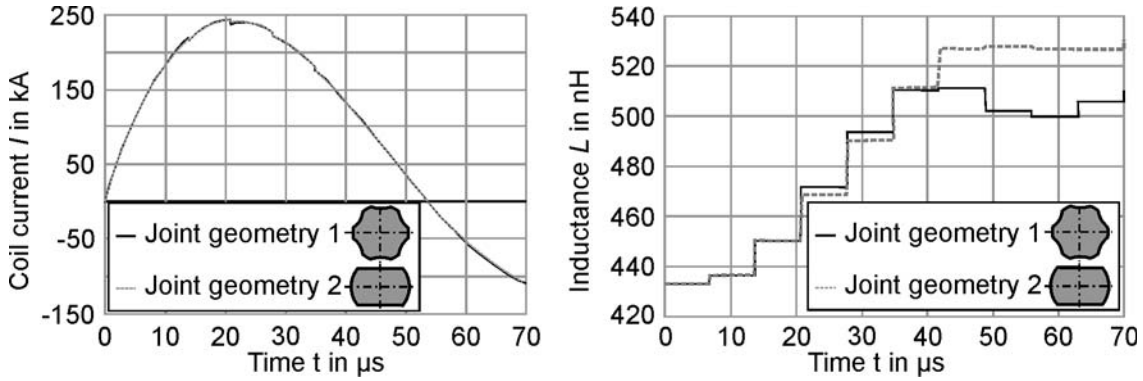

Figure 6*: Left: Coil current in the EM forming simulation. The electromagnetic simulation stops at 70µs because of the completed EM forming step and continues with the torque simulation step. Right: Inductance over the EM forming step time.*

4 Experimental Verification

The simulation was verified by an electromagnetic joining tests and subsequent static torque test for the two geometries showing the best performance in the simulation. For EMF a compression coil from Poynting GmbH with a maximum allowable voltage of 16kVwas applied. The torque test was performed on a test stand of the TU-Chemnitz with measurement of the joint torsion angle and the moment.

The simulations show good agreement to the experiments. Joint geometry 1 was not fully shaped in the experiment what was already expected through the simulation. Failure due to cracks occurs for both joint geometries on regions which already show high plastic strains in the simulation. For instance on the tube on relatively sharp edges of the shaft geometry up to ε_{eff}^{p} =0.27 for joint geometry 1 or 0.38 for joint geometry 2 exceeding the quasistatic ultimate strain for C35E significantly. The failure mode in the simulation

and in the experiment match each other and even quantitatively the achievable torques in the experiments are in good agreement with the simulation.

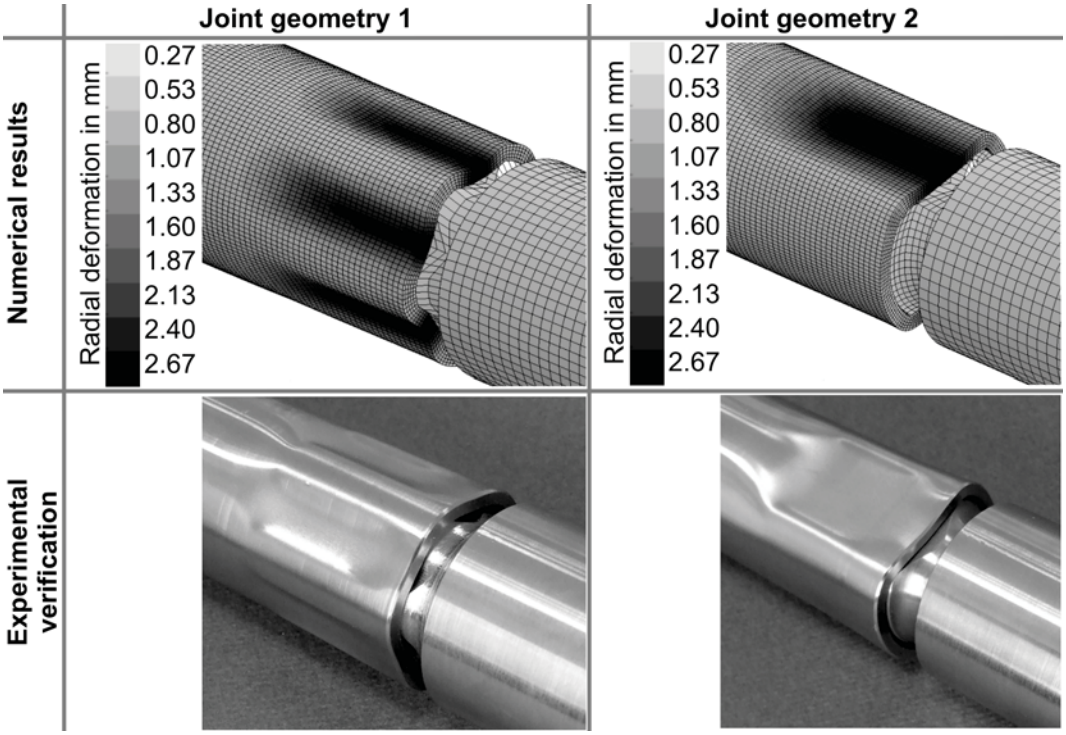

***Figure 7**: Radial deformation of the workpiece for both joint geometries (left: geometry 1, right: geometry 2) and the experimental results (bottom).*

The deviation is less than 8%, which is an acceptable value because in the simulation problems like overestimated rebound or uncertainties in friction coefficients are difficult to handle. Moreover a relation between the internal strain energy and the achievable torque could be deduced. Joint geometry 1 has an 18% higher strain energy compared with geometry 2 thus we can conclude that the higher the internal strain energy of a joint the higher the achievable loads. The magnitude of local strains is not a precise criterion. The maximum plastic strain of joint geometry 1 is even less then in case of joint geometry 2.

Specimen	Achievable moment [Nm]		Failure part	
	Simulation	Experiment	Simulation	Experiment
Joint geometry 1	2300	2408	tube	tube (crack)
Joint geometry 2	1500	1415	tube+shaft deform.	tube (crack) +shaft deform.

***Table 2:** Achievable torsion moments*

5 Conclusion and Outlook

The 3-D coupled electromagnetic-structural simulation shows a great capability for simulations of the EMF process. In particular it is the FEM-BEM method in LS-DYNA's EM

module which is perfectly suited because of advantages like no air/insulator mesh. One drawback is that large-scale problems must be handled with parallel processing due to the high computational cost or memory requirements (here 35GB for EM system). Computations considering the permeability of steel materials show, that a disregard is quite acceptable in general for EMF forming simulations. The experiments show that an optimization of the joint geometry is necessary to avoid regions of plastic strain peaks which are accountable for crack initiation. One possibility to reduce high local plastic strains is to round the sharp edges on the longitudinal grooves.

References

[1] Bühler, H., von Finckenstein, E., 1971. Bemessung von Sickenverbindungen für ein Fügen durch Magnetumformung, 104. Werkstatt und Betrieb, 45–51.

[2] Psyk, V., Risch, D., Kinsey, B.L., Tekkaya, A.E., Kleiner, M., 2011. Electromagnetic forming - a review. Journal of Materials Processing Technology 211, 787–829.

[3] Neugebauer, R.; Bouzakis, K.-D.; Denkena, B.; Klocke, F.; Sterzing, A.; Tekkaya, A.E.; Wertheim, R.: Velocity effects in metal forming and machining processes. Annals of the CIRP Vol. 60/2/2011.

[4] Weddeling, C., Woodward, S., Marré, M., Nellesen, J., Psyk, V., Tekkaya, A.E., Tillmann, W., 2011. Influence of Groove Characteristics on Strength of Form-fit Joints. Journal of Materials Processing Technology 211 (5), 925–935.

[5] Takata, N.; Kato, M.; Sato, K.; Tobe, T.: High-speed forming of metal sheets by electromagnetic forces. Japan Soc. Mech. Eng. Int. Journal 31, pp. 142-150, 1988.

[6] Kleiner, M.; Brosius, A.: Determination of Flow Curves at High Strain Rates using the Electromagnetic Forming Process and an Iterative Finite Element Simulation Scheme, Annals of the CIRP Vol. 55/1/2006.

[7] Prof. Dr. L. W. Meyer et al: Werkstoffverhalten bei hohen Dehnungsgeschwindigkeiten. Oral presentation, Workshop Impulsumformung, IUL Dortmund, 12.03.2009.

[8] Taebi, F.; Demir, K.; Stiemer, M.; Psyk, V. Kwiatkowski, L.; Brosius, A.; Blum, H.; Tekkaya, A. E.: Dynamic forming limits and numerical optimization of combined quasi-static and impulse magnetic forming. Comp. Mat. Sc. 54 (2012), pp 293-302.

[9] L'Eplattenier, et. al. Introduction of an Electromagnetism Module in LS-DYNA for Coupled Mechanical-Thermal-Simulations, steel research int. 80 (2009), No. 5

[10] http://users.physik.fu-berlin.de/~herold/HYS.pdf., 01.2012

[11] http://www.ndt.net/article/dgzfp03/papers/p12/p12.htm, 01.2012

[12] Rieben, R.N., Rodrigue, G.H., White, D.A., A high order mixed vector finite element method for solving the time dependent Maxwell equations on unstructured grids. J. of Com. Phys. 204 (2005), pp. 490-519.

[13] Castillo, P., Rieben, R., White, D., FEMSTER: An Object-Oriented Class Library of High-Order Discrete Differential Forms. In: Transactions on Mathematical Siftware, ACM, Vol. 31, No. 4, Dec. 2005, pp. 425-457.

[14] Bíró, O., Preis, K., On the Use of the Magnetic Vector Potential in the Finite Element Analysis of Three-Dimensional Eddy Currents. In: IEEE Trans. on Magn., Vol. 25 1989.